

Strong Lateral Electron Coupling of Pb Nanowires on Stepped Si(111): Angle-Resolved Photoemission Studies

Keun Su Kim, Harumo Morikawa, Won Hoon Choi, and Han Woong Yeom*

Institute of Physics and Applied Physics and Center for Atomic Wires and Layers, Yonsei University, Seoul 120-749, Korea

(Received 31 May 2007; published 8 November 2007)

We employ angle-resolved photoemission to characterize the electronic band structure of the Pb “nanowire” array self-assembled on a stepped Si(111) surface. Despite the highly oriented nanowires observed in scanning tunneling microscopy images, we find essentially two-dimensional Fermi contours modulated one dimensionally perpendicular to the wires. This strong two-dimensional and quasi-one-dimensional nature of the band structure explains the stability and anisotropy of the metallic phase down to 4 K as reported recently. A simple tight-binding model with each Si nanoterrace covered by a densely packed Pb overlayer successfully reproduces this modulated band structure and quantifies the electron coupling within the “nanostripes” and the step-edge potential.

DOI: [10.1103/PhysRevLett.99.196804](https://doi.org/10.1103/PhysRevLett.99.196804)

PACS numbers: 73.20.At, 68.43.Hn, 71.15.-m, 79.60.Dp

Low-dimensional electronic systems exhibit exotic quantum phenomena, such as charge and spin density waves, non-Fermi liquid behavior, and recently massless Dirac particles, through enhanced many-body interactions [1–3]. In particular, self-assembled atomic-scale wires on silicon surfaces, In/Si(111), Au/Si(557), Au/Si(557), and Au/Si(553), have been shown to exhibit well-defined one-dimensional (1D) metallic band structures [4–8] and served for the observation of interesting and intriguing 1D physics such as multiple Peierls instabilities [9], real-space fluctuations near a Peierls transition [10], and Rashba spin-splitting of a 1D band [11].

While the central issues in these metallic wire systems are related to the instability of their metallic phases [6–9,12], a recent study of Pb nanowires on a stepped Si(111) surface, Si(557), revealed a distinctive temperature-dependent conductivity, a stable 1D metallic conductivity down to 4 K after an abrupt transition from 2D behavior at 78 K [13]. The metallic conductivity of the nanowires at a very low temperatures is very surprising considering the possibility of Peierls instabilities [14], non-Fermi liquid behavior [15], and localization transitions [16]. If this system really has a well-defined 1D metallic behavior at a temperature as low as 4 K, it could open up the possibility of studying low-energy excitations of 1D metallic electrons in real space and with atomic resolution using scanning tunneling microscopy (STM) and spectroscopy.

In this Letter, we investigate directly the electronic band dispersions and Fermi surfaces of well-ordered Pb nanowires on Si(557) with angle-resolved photoemission (ARP) using samples characterized by STM and low-energy-electron diffraction (LEED). The ARP study reveals the following unexpected aspects concerning the electronic structure of this system; (i) the electron bands are basically 2D and the electrons can propagate across the steps between the wires and (ii) the interaction of electrons with the step(wire) superlattice induces a modulation of the 2D bands to yield poorly nested quasi-1D bands. The tight-

binding analysis indicates that the Pb nanowires are composed of a dense Pb layer covering the narrow terraces in apparent contrast to the STM images that only show a single-atomlike chain for each wire. The stability of the metallic phase as well as the anisotropic conductivity can be explained by the coexisting 2D and quasi-1D nature of the band structure.

The wire structures were characterized using a commercial low-temperature STM (Unisoku, Japan). The STM head and the sample were cooled by liquid nitrogen down to 78 K. For the ARP measurements high-performance electron analyzers (Gammadata, Sweden) were used with both He discharge radiation ($h\nu = 21.2$ eV) and synchrotron radiation ($h\nu = 140$ eV) at Pohang Accelerator Laboratory. The mapping of the Fermi surfaces and the band dispersions was performed at 70 K by rotating the sample along two orthogonal polar axes. The angle and energy resolution was 0.15° and 15 meV at best. LEED optics were available on all three experimental stations and were used to check the surface order and ensure comparable and consistent samples.

A vicinal Si(557) wafer with a 9.5° miscut from [111] was cleaned thermally. After depositing about two monolayers (ML) Pb and subsequent annealing to remove the excess Pb, a series of phases was observed as recently reported [17]. The most prominent 1D phase, the so-called $\alpha \times 2$ phase with a $4\frac{2}{3} \times 2$ periodicity [referred to Si(111) 1×1], forms at 620–640 K with a Pb coverage slightly over 1 ML [17]. The real-space image [Fig. 1] taken by STM directly reveals a well-ordered and quite regular nanowire array, where each wire appears as a line of bright protrusions with a $2a_{\text{Si}}$ periodicity [$a_{\text{Si}} = 0.384$ nm, the Si(111) 1×1 lattice constant]. The interwire spacing ($a_{\text{Si}} \times 4\frac{2}{3}$ or 1.57 nm) is explained by the formation of a (223) facet, which is composed of a step edge ($a_{\text{Si}} \times \frac{2}{3}$ width) and a (111) terrace of four Si rows ($a_{\text{Si}} \times 4$ width) as shown in Figs. 1(c) and 2(c) [18]. The earlier STM study found a disordered or incommensurately

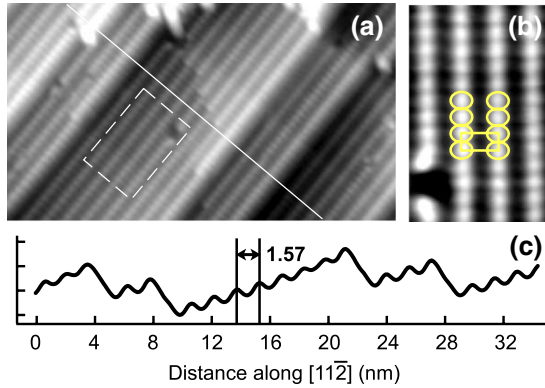


FIG. 1 (color online). (a) STM topograph of the well-ordered Pb nanowires on Si(557) at 78 K with +0.5 V sample bias over an area of $40 \times 22 \text{ nm}^2$, (b) enlarged image of the area within the dashed box in (a), and (c) height profile along the white line in (a).

modulated structure along the wires in this temperature range [13]. However, our high-resolution STM images [Fig. 1(b)] have a uniform periodic $4\frac{2}{3} \times 2$ appearance under all bias conditions. This is consistent with the sharp LEED pattern [Fig. 2(a)].

Figure 3(a) shows constant-energy contours of photoelectrons at the Fermi level in momentum space measured by ARP for Pb nanowires at 70 K. One can readily identify sixfold multiple Fermi contours (FCs) labeled as $m1$ – $m6$ within a $4\frac{2}{3} \times 1$ surface Brillouin zone (SBZ). The closed elliptical FCs of $m1$ and $m6$ are found to be centered at \bar{M} and $\bar{\Gamma}$, respectively, while the $m2$ – $m5$ FCs between them are open wavy lines. No apparent $\times 2$ periodicity along $[1\bar{1}0]$ (x axis in the figure) is observed in contrast to the STM images as discussed below.

To trace the band dispersions underlying the $m1$ – $m6$ FCs, detailed photoelectron energy-distribution curves (maps) were measured along a few high symmetry directions [Figs. 3(b)–3(d)]. The correspondence between the

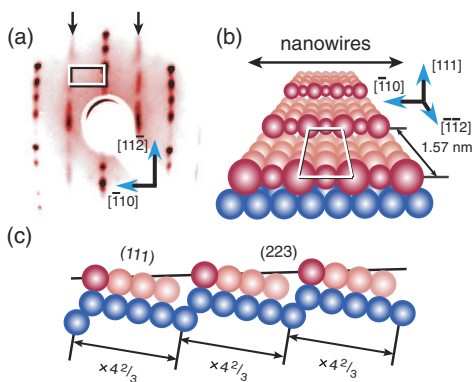


FIG. 2 (color online). (a) LEED pattern of the Pb nanowire phase at 70 K at 81 eV electron energy. (b) Front and (c) side views of the schematic model of the Pb nanowire structure; the red (blue) balls represent Pb (Si) atoms. The $4\frac{2}{3} \times 2$ unit cell is indicated by the white boxes.

FCs and the bands is further confirmed by the momentum distribution curves (blue lines) at the Fermi level. In the energy-distribution maps along the nanowires (k_x) of Figs. 3(b) and 3(c), the corresponding bands $m1$ – $m6$ can be identified clearly by their strong parabolic dispersions with their common minima on the zone boundary at a binding energy of 0.6–0.7 eV. Based on the inward (outward) dispersion of the $m1$ ($m6$) band from the center of its FC, we can identify that this FC corresponds to an electron (hole) pocket. In strong contrast, these bands have only small sinusoidal dispersions across the wires (along k_y) as shown in Fig. 3(d). All these bands can be unambiguously assigned to surface states localized on the topmost (Pb and/or Si) layers, since they are located within the Si bulk band gap, the dispersion is independent of the photon energy, and they exhibit a $\times 4\frac{2}{3}$ surface periodicity. There are at

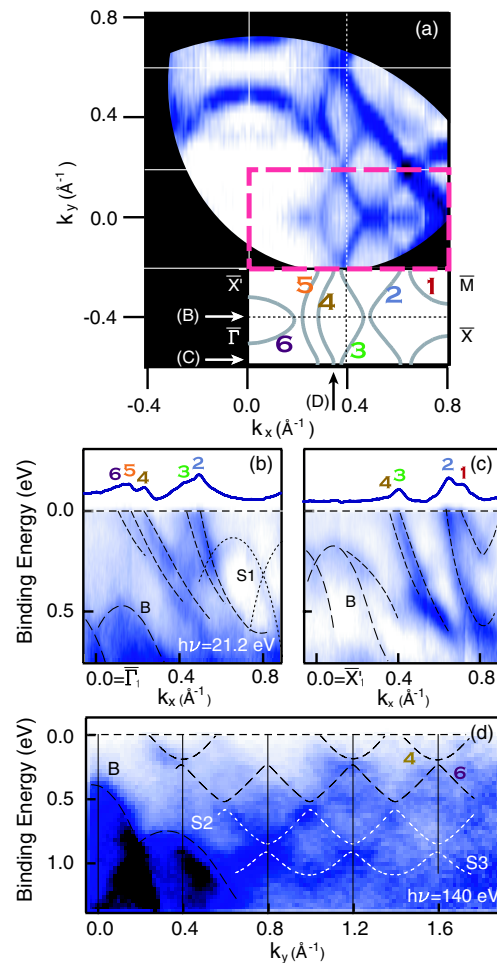


FIG. 3 (color online). ARP data of (a) Fermi surfaces and underlying band dispersions (b), (c) along and (d) perpendicular to the Pb nanowires at 70 K with photon energies of 21.2 eV and 140 eV (darker contrast for higher intensity). The schematics of the FCs within a half unit cell are given together in (a) and the arrows indicate the measured k -space lines for (b)–(d). The blue lines on top of (b), (c) are the momentum distribution curves at Fermi level and the dashed lines in (b)–(d) are guides to the eye.

least three more surface-state bands (S1–S3) within the band gap, which are fully occupied with a binding energy larger than 0.2 eV. These insulating bands are not discussed further here.

Figure 4 reveals that the complex FCs are composed of two simple basic building blocks—a circle and a rounded diamond repeating with $4\frac{2}{3} \times 1$ periodicity. As shown in the bottom of Fig. 4, the diamond explains $m1$ – $m4$ bands and is an electron pocket while the circle corresponds to the $m5$ and $m6$ bands and is a hole pocket. To our surprise, the whole electronic band structure of the surface is basically 2D with an extra 1D modulation following the periodicity of the wire array (or the step array). The overlap of the bands (FCs) in the wire-perpendicular direction produces the anticrossing gaps, which separate the FCs into the ellipses (2D bands) and wavy lines (quasi-1D bands). We will focus on the origin of the 2D bands (the circular and diamond-shaped FC) first and return to the interwire 1D modulation later.

The unexpected 2D FCs can be explained by a simple tight-binding model considering only nearest-neighbor hopping and in-plane p orbitals. We take the simplest possible lattice of a square or hexagon with the lattice constant of $\text{Si}(111)1 \times 1$. Although both lattices reproduce the diamond-shaped electron pocket, the extra circular hole pocket is unique to the square lattice. Note that a free-electronlike circular FC is gradually nested into a diamond

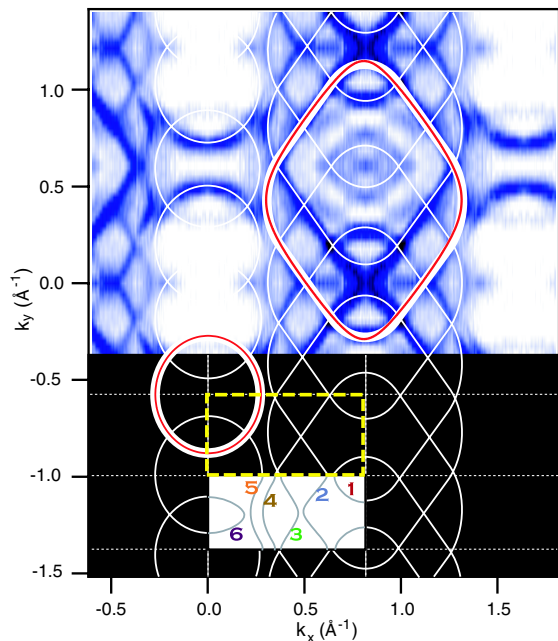


FIG. 4 (color online). The symmetrized map from the raw Fermi surface data of Fig. 3(a) showing a wider k space. The raw data taken over one quadrant ($k_x, k_y \geq 0$) of the k space are mirror symmetrized across x and y axes with subsequent translational operations. The diamond-shaped and circular contours in white or red lines are those calculated by a tight-binding model. The schematics of the experimental data are shown in the white box with $m1$ – $m6$ bands tagged by numbers.

as the electron filling approaches one half for a square or hexagonal lattice [19], which is the 2D analog of the well-known Su-Schrieffer-Heeger model [20]. The nearest-neighbor interactions within the square lattice, along (overlap integral γ_x) and perpendicular (γ_y) to the wires, were optimized next to simulate the observed FCs quantitatively. The final result is shown in Fig. 4 (red lines), in excellent agreement with experiment. The ratio of the interactions (γ_x/γ_y) is found to be 1.2, i.e., the nearest-neighbor electron coupling is very isotropic and 2D.

The tight-binding analysis indicates that the sample surface is covered by a dense Pb layer with a 1×1 square unit cell. This is in contradiction to the STM images which apparently reveal wires consisting of a single atomic chains. The formation of a dense Pb layer, however, is consistent with a recent core-level photoemission result [17] and the coverage estimate (1.0–1.3 ML) [13,17]. This apparent discrepancy can be understood from the fact that the STM imaging of a vicinal surface often picks up the step-edge structure preferentially with very little contrast from atoms within the terraces [4,9,21]. Thus, the structural model of the Pb nanowire phase must be as shown in Figs. 2(b) and 2(c); the dense 1×1 Pb rows (only three rows are possible) in each terrace with a step-edge Pb row. The step-edge Pb row can either be a single-atom row with a $\times 2$ modulation forced probably by a step-edge Si reconstruction or that with extra Pb adatoms decorating alternate unit cells. The latter seems more plausible considering the enhanced contrast of the step-edge chains in STM and the coverage larger than 1 ML [18]. The present system, thus, can be more properly described as Pb *nanostripes* separated by Si steps and the electronic band structure is mainly governed by the *invisible* Pb rows within the narrow terraces. Some electronic difference of the edge Pb row might be expected but no corresponding electronic state is identified at least near the Fermi level. This model also naturally explains the lack of an apparent $\times 2$ periodicity in the FCs and band dispersions since most of the Pb atoms are located within the terrace and not significantly perturbed by the modulation along the step-edge rows.

The original 2D FCs described above are, however, modulated by the periodic nanostripe (or step) array [see Fig. 4]. This is similar to the case of the formation of electronic superlattice states on vicinal metal surfaces [22–24], where the 2D electronic states on the surfaces are modulated by 1D periodic potentials of regular step arrays. It indicates that the electrons of the Pb nanostripes are not tightly confined but propagate rather easily over the steps. The degree of electron confinement within the narrow terraces is determined by the strength of the effective step potential but a large variation of the step potential was observed on vicinal metal surfaces [22–24]. That is, the terrace electrons can either be strongly confined to form 1D quantum well states laterally or be rather well delocalized over the steps. This phenomenon can be easily modeled by

a 1D periodic potential. A fit to the sinusoidal band dispersions perpendicular to the wires shown in Fig. 3(d) quantifies the effective step potential as 60 ± 5 meV, which is quite small. In contrast, a recent study on a 2D Ag monolayer on Si(111) gave the monoatomic step potential as 4.5 ± 2.5 eV [25], which is 2 orders of magnitude larger than the present case. We note that the large variation of the effective step potential on vicinal metal surfaces was suggested to be related to the terrace width [22–24]. However, the origin of such a huge difference in the effective step potential is not clear yet and further studies are required including detailed structural studies for step edges with different adsorbates.

In comparison to the step-superlattice states on vicinal metal surfaces [22–24], the unique feature of the present system is that the Fermi wave vector of the original 2D bands is much larger than the step-superlattice vector [Fig. 4]. It makes the FCs overlap mutually and split into the multiple quasi-1D and 2D bands as small anticrossing gaps open. This yields the peculiar intermixed dimensional character of the band structure with quasi-1D bands ($m2$ – $m5$) delocalized preferentially along the wires and the 2D bands ($m1$ and $m6$). Qualitatively speaking, this unique and anisotropic band structure can produce the anisotropic conductivity [13], which is basically due to the step potential quantified above. On the other hand, the electrons in each nanowire (nanostripe) are still not perfectly confined and can rather easily hop across the steps due to the small step potential. This makes the electronic states near Fermi level far from being strictly 1D with poorly nested FCs. Thus, the stable metallic phase at low temperature [13] overcoming Peierls instability can reasonably be understood. Quantitatively speaking, the band anisotropy (ratio of the bandwidths along and across the wires) of the quasi-1D bands of the present system, not to mention the 2D electron ($m1$) and hole ($m6$) pockets, is as small as 3–7 [3.09 ($m2$), 4.13 ($m3$), and 6.13 ($m4$)] in clear contrast to the large anisotropy of 50–70 for the other metallic wire systems on flat and vicinal Si(111) surfaces featuring Peierls instability at 130–270 K [6–9,12].

However, the reason for the abrupt change of conductivity observed around 78 K [13] is not clear. We did not find any change in the band structure and STM images around this temperature. Although Tegenkamp *et al.* discussed the role of an extra long-range modulation along the step-edge rows [13], we did not observe any such modulation in our STM images. While this discrepancy needs further investigation, we suggest that the temperature-induced crossover from 1D to 2D conductivity may be explained by the onset of the interwire conduction overcoming thermally the effective step potential of 60 meV.

In summary, we used ARP to characterize the electronic band structure of a Pb nanowire array self-assembled on a stepped Si(111) surface. We observe essentially 2D bands,

which are modulated one dimensionally due to the array of wires. The 2D bands arise from the dense Pb stripes covering each terrace and the 1D modulation originates from the periodic step potential. The mixed 2D and quasi-1D nature of the band structure explains qualitatively the stability and anisotropy of the metallic phase at low temperature. Further studies on the electronic and transport properties of this *nanowire array* with mixed dimensionality would be very interesting.

This work was supported by KOSEF through the Center for Atomic Wires and Layers of the CRi program. P. A. L. was supported by MOST of Korea and POSCO.

*yeom@yonsei.ac.kr

- [1] George Grüner, *Density Waves in Solids* (Addison-Wesley, Reading, MA, 1994).
- [2] J. M. Luttinger, *J. Math. Phys. (N.Y.)* **4**, 1154 (1963).
- [3] A. K. Geim and K. S. Novoselov, *Nat. Mater.* **6**, 183 (2007).
- [4] J. N. Crain *et al.*, *Phys. Rev. Lett.* **90**, 176805 (2003).
- [5] J. N. Crain *et al.*, *Phys. Rev. B* **69**, 125401 (2004).
- [6] H. W. Yeom *et al.*, *Phys. Rev. Lett.* **82**, 4898 (1999).
- [7] J. R. Ahn, H. W. Yeom, H. S. Yoon, and I.-W. Lyo, *Phys. Rev. Lett.* **91**, 196403 (2003).
- [8] J. R. Ahn, H. W. Yeom, E. S. Cho, and C. Y. Park, *Phys. Rev. B* **69**, 233311 (2004).
- [9] J. R. Ahn, P. G. Kang, K. D. Ryang, and H. W. Yeom, *Phys. Rev. Lett.* **95**, 196402 (2005).
- [10] S. J. Park, H. W. Yeom, J. R. Ahn, and I.-W. Lyo, *Phys. Rev. Lett.* **95**, 126102 (2005).
- [11] I. Barke, F. Zheng, T. K. Rügheimer, and F. J. Himpsel, *Phys. Rev. Lett.* **97**, 226405 (2006).
- [12] P. C. Snijders, S. Rogge, and H. H. Weitering, *Phys. Rev. Lett.* **96**, 076801 (2006).
- [13] C. Tegenkamp *et al.*, *Phys. Rev. Lett.* **95**, 176804 (2005).
- [14] T. Tanikawa, I. Matsuda, T. Kanagawa, and S. Hasegawa, *Phys. Rev. Lett.* **93**, 016801 (2004).
- [15] M. Bockrath *et al.*, *Nature (London)* **397**, 598 (1999).
- [16] E. Abrahams, S. V. Kravchenko, and M. P. Sarachik, *Rev. Mod. Phys.* **73**, 251 (2001).
- [17] K. S. Kim, W. H. Choi, and H. W. Yeom, *Phys. Rev. B* **75**, 195324 (2007).
- [18] H. Morikawa, K. S. Kim, D. Y. Jung, and H. W. Yeom, *Phys. Rev. B* **76**, 165406 (2007).
- [19] Q. Yuan, T. Nunner, and T. Kopp, *Eur. Phys. J. B* **22**, 37 (2001).
- [20] A. J. Heeger, S. Kivelson, J. R. Schrieffer, and W.-P. Su, *Rev. Mod. Phys.* **60**, 781 (1988).
- [21] H. W. Yeom *et al.*, *Phys. Rev. B* **72**, 035323 (2005).
- [22] A. Mugarza and J. E. Ortega, *J. Phys. Condens. Matter* **15**, S3281 (2003).
- [23] F. Baumberger *et al.*, *Phys. Rev. Lett.* **92**, 196805 (2004).
- [24] F. Baumberger *et al.*, *Phys. Rev. Lett.* **92**, 016803 (2004).
- [25] I. Matsuda *et al.*, *Phys. Rev. Lett.* **93**, 236801 (2004).